

Article

Fabrication of a PLA/PVA-BIO-HA Polymeric Membrane by the Electrospinning Technique

Brenda Lizbeth Arroyo-Reyes ^{1,*}, Celia Lizeth Gómez-Muñoz ², Plácido Zaca-Morán ², Fabián Galindo-Ramírez ¹ and Marco Antonio Morales-Sánchez ³

¹ Instituto de Fisiología, Benemérita Universidad Autónoma de Puebla, Puebla C.P. 72570, Mexico; fabian.galindo@correo.buap.mx

² Instituto de Ciencias, Benemérita Universidad Autónoma de Puebla, Puebla C.P. 72050, Mexico; celia.gomez@correo.buap.mx (C.L.G.-M.); placido.zaca@correo.buap.mx (P.Z.-M.)

³ Facultad de Ingeniería Química, Benemérita Universidad Autónoma de Puebla, Puebla C.P. 72570, Mexico

* Correspondence: brenda.arroyore@alumno.buap.mx

Abstract: In the present work, the fabrication of a membrane composed of polylactic acid (PLA), polyvinyl alcohol (PVA), and Biological Hydroxyapatite (BIO-HA) is reported using the coaxial electrospinning technique. The membrane fabrication process involved mixing a solution of PLA and trichloromethane (TCM) with a second solution of PVA, isopropyl alcohol (IPA), distilled water, and BIO-HA at 110 °C. Subsequently, the electrospinning process was carried out using a voltage of 25 kV for 30 min on a rotating drum collector at 1000 rpm. The membrane was characterized through Scanning Electron Microscopy (SEM), Energy-Dispersive X-ray spectroscopy (EDS), Fourier-Transform Infrared spectroscopy (FTIR), Thermogravimetric Analysis (TGA), and Differential Scanning Calorimetry (DSC). The morphological results revealed the presence of randomly arranged fibers with an average diameter of 290 ± 9 nm and interfiber spacing ranging from 200 to 700 nm, which are characteristics conducive to cell proliferation. Additionally, FTIR studies confirmed the presence of BIO-HA and the constituent elements of the polymers in the composite membrane. The polymeric membrane in contact with human mesenchymal stem cells was characterized as showing significant differences in its behavior at 6, 24, and 72 h post-contact. These studies indicate that the membrane provides physical support as a scaffold due to its suitable morphology for cell adhesion and proliferation, attributable to the electrospinning conditions as well as the polymers contained in BIO-HA. Membrane toxicity was confirmed through a cytotoxicity study using fluorescence microscopy, which showed that the membrane provided a favorable environment for cell proliferation. These results suggest that exposure to BIO-HA enhances its potential application in bone and joint tissue regeneration.

Keywords: PLA; PVA; BIO-HA; electrospinning; membrane; biocompatibility; cytocompatibility



Citation: Arroyo-Reyes, B.L.; Gómez-Muñoz, C.L.; Zaca-Morán, P.; Galindo-Ramírez, F.; Morales-Sánchez, M.A. Fabrication of a PLA/PVA-BIO-HA Polymeric Membrane by the Electrospinning Technique. *Fibers* **2024**, *12*, 33. <https://doi.org/10.3390/fib12040033>

Academic Editor: Mazeyar Parvinzadeh Gashti

Received: 22 January 2024

Revised: 11 March 2024

Accepted: 21 March 2024

Published: 3 April 2024



Copyright: © 2024 by the authors. Licensee MDPI, Basel, Switzerland. This article is an open access article distributed under the terms and conditions of the Creative Commons Attribution (CC BY) license (<https://creativecommons.org/licenses/by/4.0/>).

1. Introduction

Biodegradable and bioabsorbable polymers, including polylactic acid (PLA), polycaprolactone (PCL), polyethylene oxide (PEO), poly(3-hydroxybutyrate) (PHB), and polyglycolic acid (PGA), have attracted considerable interest in the fields of tissue engineering, biotechnology, and regenerative medicine as potential substitutes for metallic implants. Despite the inherent drawbacks associated with each polymer on its own, there has been an observation that blending them with additional compounds leads to improved properties, thereby boosting their suitability for diverse applications. Recently, these bioabsorbable polymers have found applications in medical fields such as tissue fixation, using elements such as screws and nails designed for bones. Additionally, they have been employed in sustained drug release systems as well as in the development of dressings, promoting the wound healing process. Their notable properties include pressure resistance, absorptive

capacity, and the ability to protect against metallic corrosion. These key attributes not only have the potential to significantly improve patients' quality of life by offering more efficient and personalized medical solutions but also contribute to the sustainability and effectiveness of healthcare systems.

The studies on tissue engineering, particularly focused on membranes, have been directed towards finding materials compatible with both soft and bone tissues [1–4]. Bone scaffolds play a crucial role in restoring the anatomical and functional integrity of damaged or lost bone structures due to various causes, ranging from congenital conditions to traumas, consequences of oncological processes, and infectious conditions [5–10]. These materials are employed to replace missing bone tissue, facilitating the recovery and improvement of both mechanical function and the affected morphological structure [11,12].

Currently, various types of tissue engineering implants are being explored, such as xenografts, 3D printing, and the electrospinning technique, among others, to obtain scaffolds to serve as regeneration guides. The electrospinning technique uses electrostatic forces to fabricate polymeric fibers with diameters in the micro- and nanometric range [13–16]. This technique presents notable advantages by allowing the efficient fabrication of highly porous membranes, with precise control over parameters such as deposition time, voltage, and the type of collector used. Particularly, coaxial electrospinning, a significant variant of this technique, is frequently used to produce fibers capable of incorporating drugs [17–20] or proteins [21,22], which is crucial for achieving long-term release.

The study of BIO-HA-compatible materials has provided a deeper understanding of two polymers that play an important role in tissue engineering and the fabrication of surgical sutures. The first is polyvinyl alcohol (PVA), a biodegradable polymer known for its hydrophilic and biocompatible properties. On the other hand, PLA is a hydrophobic polyester widely used in these fields. Moreover, this polymer exhibits excellent thermal properties, processability, and gas permeability, which makes it particularly attractive for various biomedical applications [23,24].

Furthermore, PVA is hydrophilic, biocompatible, and has good processability, allowing it to be combined with HA, which is difficult to electrospun on its own. Additionally, PVA possesses hydrolytic properties that enhance mechanical properties when mixed with other hydrophobic polymers. Therefore, the combination of these materials has led to the development of polymeric membranes with reduced brittleness, increasing the strength of the fiber for tissue engineering applications. These properties enable the characteristics of PLA-PVA mixtures to be biocompatible, facilitating the release of BIO-HA through polymer degradation [25]. BIO-HA, short for biological hydroxyapatite, is a biomineral naturally found in human bones. It enhances bioactivity and biocompatibility, making it valuable in applications such as bone regeneration and dentistry. Furthermore, BIO-HA serves as an osteoinductive material that is biomimetic to the bone mineral [25].

In 2018, Alharbi, H. F. et al. reported on the study of coaxial electrospinning technique to fabricate composite nanofibers with a PLA core and an outer layer of PVA [26]. SEM results showed that the PVA/PLA nanofibers exhibit a fiber spacing structure with diameters of 138 nm and 165 nm. Additionally, their studies demonstrated that the composite nanofibers exhibited higher hydrophilicity and a significant improvement in strength and stretching capacity compared to pure PLA. Moreover, the fabricated nanofibers showed compatibility in experiments with the growth and adhesion of human embryonic kidney cells (HEK-293). These results demonstrate the potential of PLA/PVA composite nanofibers for biomedical applications and tissue regeneration.

Li, T. T. et al. reported in 2020 on the study of braided bone scaffolds using composite fibers of PLA and PVA [27]. The resulting braided filaments, previously thermally treated, were used as matrices for the fabrication of bone frameworks through the electrodeposition of hydroxyapatite (HA) using titanium (Ti) electrodes. SEM, tensile-deformation, and EDS results showed that, at a PLA/PVA ratio of 3:1, the braids exhibit maximum deformation properties and a structural and morphological spacing with active sites for HA incorpora-

tion by electrodeposition. In vitro results through immersion in simulated body fluid (SBF) demonstrated that this treatment is biocompatible for applications in spongy bone repair.

Furthermore, a recent study introduced a silver-containing gel based on polyvinyl alcohol and aryloxycyclotriphosphazene containing β -carboxyethenylphenoxy and p-formylphenoxy groups [28]. The gel was evaluated in a rabbit model to inhibit the growth of the main microorganisms in contact with their skin: the bacteria *S. aureus*, *P. aeruginosa*, *E. coli*, *B. subtilis*, *S. epidermidis*, and *C. stationis*, and the fungus *C. albicans*. The study of the wound-healing effect of the gel in vivo showed a decrease in the wound area of the rabbit hind limb by 91.43% ($p < 0.05$) on the 10th day of observation.

In this work, the fabrication of a PLA/PVA-BIO-HA composite membrane obtained through coaxial electrospinning is reported. This membrane shows the morphology of fibers with random orientation and submicrometric diameters. FTIR spectroscopy studies confirmed the presence of functional groups associated with PLA, PVA, and BIO-HA based on the morphological, compositional, and cytotoxicity assay results, the composite membrane exhibited excellent cell adhesion and biocompatibility. This suggests its potential application in fields such as healthcare and tissue engineering, where it could play a crucial role in bone tissue regeneration.

2. Materials and Methods

2.1. Preparation and Characterization of the BIO-HA

In this work, the synthesis of BIO-HA was carried out using the bovine bone calcination technique, following the methodology detailed by Fernández-Cervantes et al. [29]. The process involved cleaning a bovine bone by exposing it to water at 100 °C for 1 h, followed by immersion in a 1:1 solution of acetone and ethanol for 30 min. This procedure was performed to eliminate the adipose tissue from the surface of the bone tissue. Subsequently, excess water and fibrous tissue were removed through a drying process in a furnace at 60 °C for 20 h. The material was then thermally treated at 900 °C for 6 h. Finally, a manual grinding process was carried out using a mortar to obtain BIO-HA particles.

The morphology of BIO-HA particles was examined using a scanning electron microscope (SEM, model JSM-6610LV Jeol, Akishima, Tokyo, Japan) with secondary electron detection, an acceleration voltage of 20 kV, and a magnification of 2000 \times . The characterization of the crystal structure was performed using an X-ray diffractometer (D8-Discover Bruker, Karlsruhe, Germany) in a grazing incidence mode (GIXRD), with CuK α radiation ($\lambda = 1.54 \text{ \AA}$) in the range of 20 to 60°. To identify the functional groups of BIO-HA, a spectrophotometer (model Vertex 70, Bruker, Karlsruhe, Germany) was employed in the mid-infrared region from 4000 to 400 cm^{-1} with a resolution of 4 cm^{-1} in attenuated total reflection (ATR) mode.

2.2. Fabrication and Characterization of the Composite Membrane (PLA/PVA-BIO-HA)

A homogeneous PLA solution was prepared by dissolving 0.8 g of PLA filament fragments used for 3D printing (COLOR PLUS[®], Ciudad de México, México, $\phi = 1.75 \text{ mm}$, industrial grade) in 10 mL of trichloromethane (TCM) at a constant temperature of 90 °C for 90 min with continuous stirring. The selection of this material is due to its frequent use in the medical field, which is attributed to its biocompatibility, renewable origin, as well as its mechanical properties and biodegradation capacity.

Additionally, a second PVA-BIO-HA solution was prepared with 2.4 g of PVA filament fragments used for 3D printing (COLOR PLUS[®], Ciudad de México, México, $\phi = 1.75 \text{ mm}$, industrial grade) in 4 mL of distilled water, 6 mL of isopropyl alcohol (IPA), and 0.8 g of BIO-HA at a constant temperature of 110 °C for 90 min with constant stirring. This polymer was chosen due to its hydrophilic nature and its ability to promote biodegradation by biological organisms. Being considered a biodegradable mimic of natural polymers, it becomes a harmless and non-toxic polymer. This choice aligns with the pursuit of environmentally sustainable materials and compatibility with biomedical applications. The incorporation of

BIO-HA into the solution imparts biomimetic properties to the membrane, enhancing its biomedical properties and functions.

The prepared solutions were used to fabricate the PLA and PVA-BIO-HA membranes using the electrospinning technique with coaxial injection of PLA/PVA-BIO-HA solutions in a 1:3 ratio. A rotating drum collector at 1000 rpm of speed was used, maintaining 11 cm between the injection head and the collector. The injection of solutions was carried out for 30 min, applying a voltage of 25 kV. The electrospun fibers were collected for 30 min on a sheet of wax paper. The advantage of the wax paper is its flexibility, allowing the fabricated fibers to be detached without causing damage.

The fabricated membranes were characterized, including the evaluation of their morphology by SEM, the identification of functional groups and structural elements through FTIR spectroscopy, and the thermal characterization by thermogravimetric analysis (TGA) and Differential Scanning Calorimetry (DSC) using NETZSCH STA 449F3 Instruments equipment. The data were obtained from 23 to 1000 °C with a heating rate of 25 °C/min in an inert nitrogen atmosphere.

2.3. Cell Proliferation Assay

The mesenchymal cells utilized in this study were extracted from the human umbilical cord, and the donors were provided by the Hospital General de Cholula, Mexico. The acquisition of these cells was carried out with proper informed consent from the donors, and the procedure was duly approved by the ethical committee of the Faculty of Medicine at BUAP. In this study, mesenchymal cells underwent trypsin/EDTA dispersion, following the methodology described by Arbós A. et al. [30]. These cells were cultivated in HAM-F12 medium with 10% fetal bovine serum (FBS) under an atmosphere of 5% CO₂ and 95% humidity at 37 °C. In experiments, 10,000 cells per well were seeded in 96-well plates, with the PLA/PVA-BIO-HA membrane in direct contact with the cell culture.

Cell proliferation assessment was carried out using WST-1 (Sigma Aldrich, St. Louis, MA, EE.UU.). The protocol was carried out following the manufacturer's instructions, using an ELISA (microplate absorbance reader kit) reader with exposure times of 6, 12, 24, 48, and 72 h, following the manufacturer's recommendations. Statistical analysis was performed with cellular experiments conducted in triplicate. The *t*-Student test was employed for group comparisons, and a significance level of $p < 0.05$ was considered.

At the same time, fluorescence microscopy characterization was performed using the Live/Dead kit (Sigma, Darmstadt, Germany) to study the cytotoxicity of the mixed membrane at 6, 12, 24, 48, and 72 h in contact with the cells.

3. Results and Discussion

3.1. Synthesized BIO-HA

Figure 1 shows the SEM micrograph of the synthesized BIO-HA, revealing clusters of irregularly sized particles resembling spheres, with particle sizes ranging from 0.5 to 2 µm. The closely spherical-shaped particles are the most common morphology for this material. From the SEM analysis, we can observe that the particles formed were highly agglomerated.

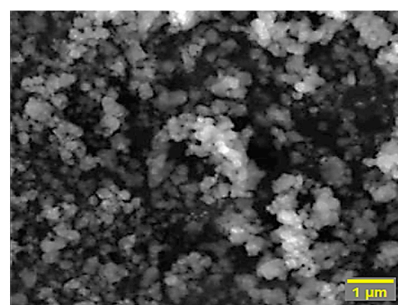


Figure 1. SEM micrograph of BIO-HA obtained by the bovine bone calcination technique.

The diffraction pattern of BIO-HA is shown in Figure 2a, which shows characteristic peaks indexed to the planes (010), (002), (211), (112), (300), (310), (222), and (213), corresponding to the compact hexagonal structure of hydroxyapatite (PDF No: 9-432).

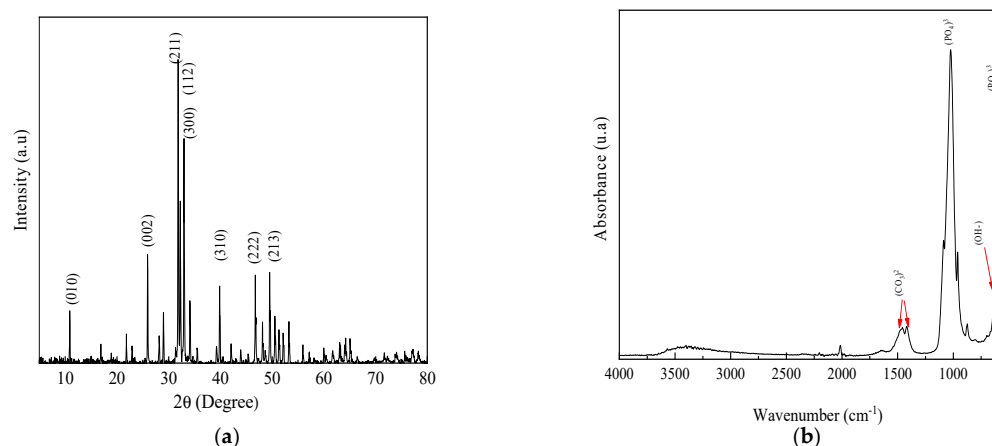


Figure 2. (a) X-ray diffraction pattern of BIO-HA; (b) FTIR spectrum of BIO-HA.

The FTIR spectrum shown in Figure 2b shows the presence of characteristic functional groups of BIO-HA, showing a band at 636 cm^{-1} corresponding to bending vibrations of OH functional groups of BIO-HA. Additionally, characteristic bands of bending vibrations of the $(\text{PO}_4)^{3-}$ functional group were identified at 1033, 957, 603, and 566 cm^{-1} , along with the presence of bands at 1539, 1458, and 1413 cm^{-1} , indicative of the carbonate group $(\text{CO}_3)^{2-}$ [31,32].

3.2. Polymeric Electrospinning Membranes

The morphological analyses through SEM of the membranes obtained from PLA and PVA-BIO-HA are presented in Figure 3. The PLA membrane shown in Figure 3a, shows a heterogeneous distribution of ribbon-like fibers with pores, characterized by a non-uniform spacing of approximately $\sim 1.8 \pm 2\ \mu\text{m}$ between them. In contrast, when the BIO-HA was added thinner fibers were obtained. The PVA-BIO-HA membrane (Figure 3b) shows a random distribution of mostly cylindrical fibers of $\sim 0.51 \pm 8\ \mu\text{m}$ in diameter. This decreasing effect on the fiber diameter can be attributed to the hydrophilic nature of the PVA, which prevents the complete evaporation of solvent, allowing the polymer jet to undergo proper stretching and solidification during its flight to the collector [33]. Also, smaller fiber spacings were compared to PLA membranes. Additionally, some nodules are observed in some sections of the fibers, which could be related either to the high concentration of PVA that can have a significant effect on the transformation of a solution droplet at the needle tip into a charged uniaxial jet [33] or to the fact that the viscosity of the PVA solution did not overcome the electrostatic repulsion, leading to the formation of separate droplets instead of forming a continuous filament [34].

Figure 4 shows the SEM micrograph and the diameter histogram of the fibers of the composite membrane. In Figure 4a, the SEM micrograph depicts a membrane with fibrous structures exhibiting a random arrangement with irregular diameters and spacings of different sizes between fibers without showing coalescence [35]. The surface of fibers is completely smooth and reveals the presence of nodules that can be attributed to the presence of PVA in the membrane and could be related to the highest concentration of the starting solution compared to the PLA solution. This also prevents polymer chain entanglements and therefore the formation of completely smooth fibers [33]. The membrane exhibits interfiber spacing of approximately $0.5\ \mu\text{m}$, with a width ranging from 200 nm to 700 nm. A second spacing range was identified, ranging from 700 nm to 1600 nm, with few gaps greater than 1700 nm. Lenhert, S. et al. reported that these membrane spacings favor nutrient diffusion, cell migration, and osteoblast cell adhesion [36]. The

statistical analysis of the diameter of the fibers that constitute the membrane is depicted in the histogram in Figure 4b, where a distribution of fiber diameters ranging from 110 nm to 941 nm can be observed, with an average diameter of 290 nm. The SEM characterization revealed a morphology with functional features that can act as a scaffold or guide for tissue regeneration, particularly in applications related to bone regeneration. It is important to mention that the surface-to-volume ratio of these electrospun membranes can be employed as scaffolds, having various benefits, such as cell adhesion [37,38].

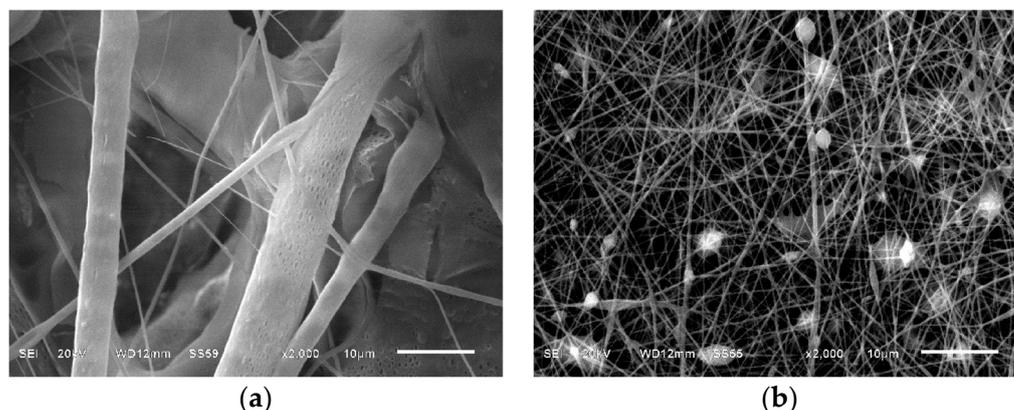


Figure 3. SEM micrographs of the electrospun membranes: (a) From the PLA solution; (b) From the PVA/BIO-HA solution.

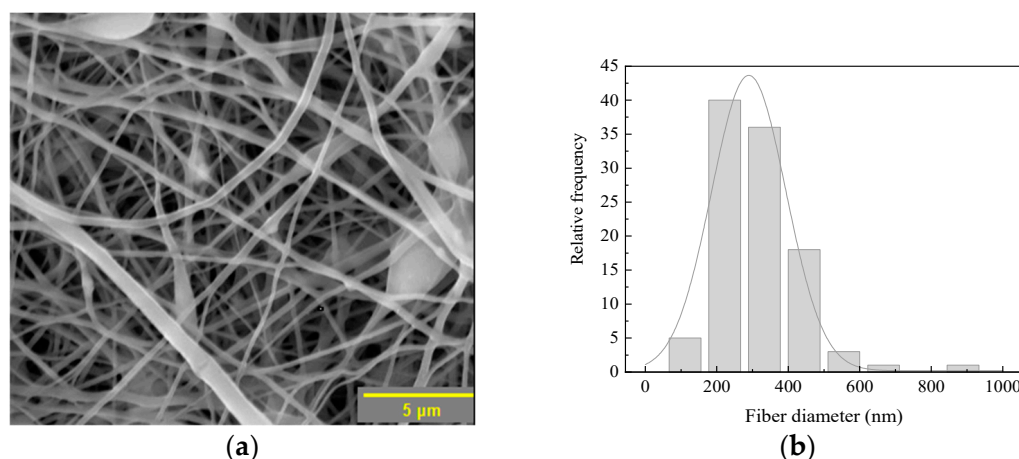


Figure 4. (a) SEM micrograph; (b) Histogram of fiber diameters of the composite membrane.

In Figure 5, the FTIR spectra obtained from PLA, PVA-BIO-HA, and PLA/PVA-BIO-HA membranes are presented. The FTIR spectrum in Figure 5a shows characteristic PLA bonds at 3300 cm^{-1} associated with OH functional groups, as well as bonds at 1745 , 1176 , and 1085 cm^{-1} assigned to the stretching vibration of the C-O group, 1456 cm^{-1} corresponding to the bending vibration of the CH bond in the CH_3 group, and 1374 cm^{-1} related to a deformation in the symmetry of the CH_3 group. Additionally, the spectrum shows a signal at 869 cm^{-1} corresponding to the stretching vibration of the C-C [34]. Figure 5b shows the characteristic functional groups of BIO-HA phosphates, along with an increase in the signal at 3300 cm^{-1} related to the stretching vibrations of OH functional groups. Furthermore, bands are observed around 2912 cm^{-1} corresponding to the stretching vibration of the CH_2 group, 1663 cm^{-1} typical of the stretching vibration of the C=O group, 1081 cm^{-1} identified with the stretching vibration of the CO group, and 834 cm^{-1} associated with the rocking vibration of the CH_2 group [39]. The FTIR spectrum in Figure 5c presents the functional groups that confirm the presence of BIO-HA and PLA-PVA polymers, demonstrating that the membrane is made up of these three compounds.

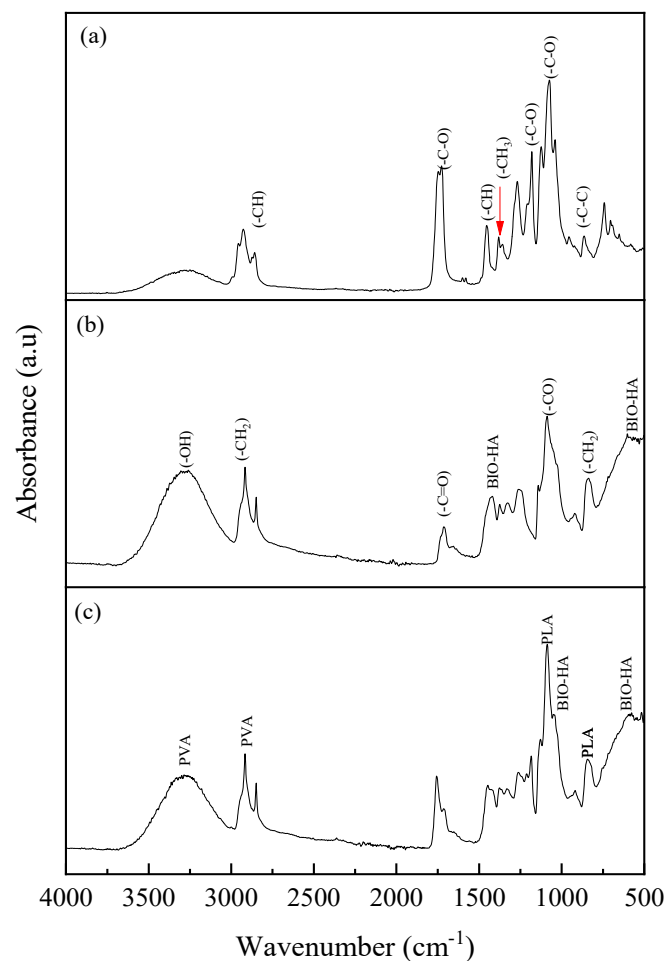


Figure 5. FTIR spectra of electrospun membranes: (a) PLA; (b) PVA-BIO-HA; (c) PLA/PVA-BIO-HA.

The thermograms of the electrospun membranes of PLA, PVA-BIO-HA, and PLA/PVA-BIO-HA are shown in Figure 6. Figure 6a shows the thermogram of the PLA membrane, where a degradation step is observed, with a T_{onset} of 332 °C, attributed to the breaking of bonds in the polymer structure leading to the release of gaseous products, such as cyclic oligomers, acetaldehyde, lactide, and carbon monoxide [40], with a residue of 0.77 wt% at 1000 °C. The thermogram of PVA-BIO-HA membrane (Figure 6b) shows two regions of weight loss: the first from room temperature to 278 °C, attributed to the loss of water or solvent residues, and the second within the interval 278–440 °C [41], with a residue of 4.92% at 1000 °C. The analysis of the thermal stability of the composite membrane PLA/PVA-BIO-HA shows a gradual decomposition process in four stages, as illustrated in Figure 6c. In the first stage, which takes place at temperatures below 100 °C, the loss is attributed to the elimination of absorbed moisture and solvents present in the membrane [39]. The second stage, which is in the range of 190 to 270 °C, is associated with the loss of low-molecular-weight substances, such as residual acetate groups, unconjugated polyenes, and water. The third stage corresponds to the loss of the main functional groups of the polymer, occurring in the range of 350 °C [40–42]. The fourth and final stage, at a temperature of 400 °C, includes the chemical elements that make up BIO-HA. With a residue of 13.2% at 1000 °C, the PLA/PVA-BIO-HA membrane exhibits higher thermal stability compared to membranes of PLA and BIO-HA. This finding suggests that the presence of BIO-HA has a positive influence on the thermal stability of the membrane, reaching its maximum decomposition temperature at 433 °C [43].

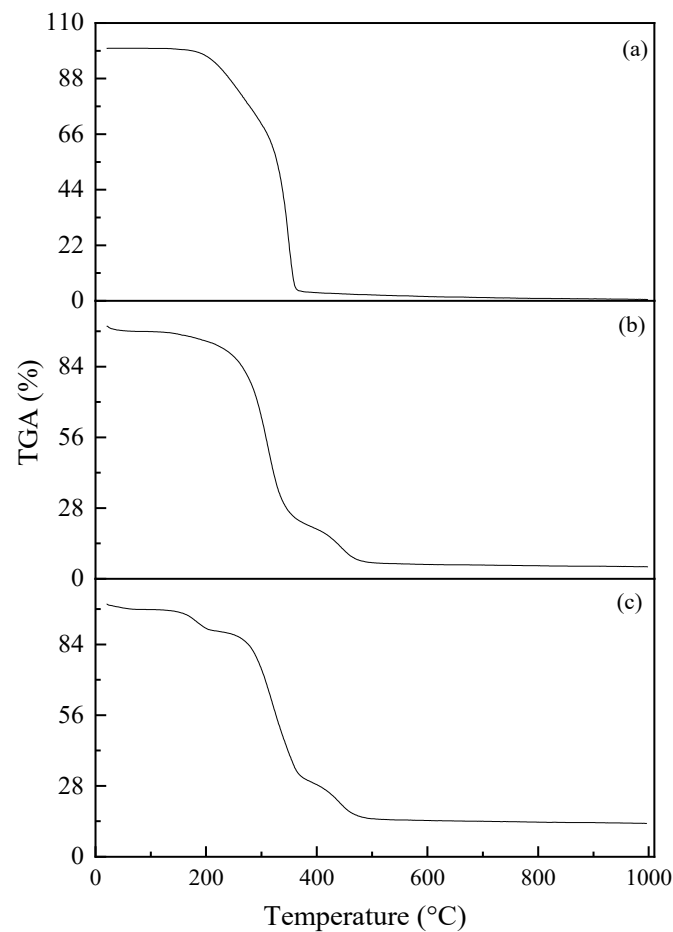


Figure 6. Thermograms of the electrospun membranes: (a) PLA; (b) PVA-BIO-HA; (c) PLA/PVA-BIO-HA.

Figure 7 shows the DSC curves of electrospun membranes. According to the DSC results of the PLA membrane (Figure 7a), the T_p of PLA is around 348 °C, corresponding to the point of the highest rate of change observed in the weight loss curve. In the case of the PVA-BIO-HA membrane (Figure 7b), the most significant weight loss occurred around 300 °C. In the case of the PLA/PVA-BIO-HA membrane (Figure 7c), the most significant weight loss is like that of the PVA-BIO-HA membrane because it happened close to 300 °C.

The values reported in Table 1 correspond to the EDS results of the composite membrane, where it is observed that the components of the PLA/PVA-BIO-HA membrane are calcium (Ca), oxygen (O), phosphorus (P), and carbon (C), of which Ca, P, and O are the main components of BIO-HA, while C is related to the polymers of the composite membrane. The stoichiometric Ca/P ratio, calculated from the weight percentage (wt%) of the composite membrane, is 2, which is below that reported for hydroxyapatite membranes [32]. This decrease could be due to the incorporation of the polymer atoms into the BIO-HA network that makes up the membrane. Figure 8 shows the representative mapping that reveals the percentage of each element identified in the analysis. It is important to mention that three different regions were analyzed to make the statistical analysis and obtain the weight percentage.

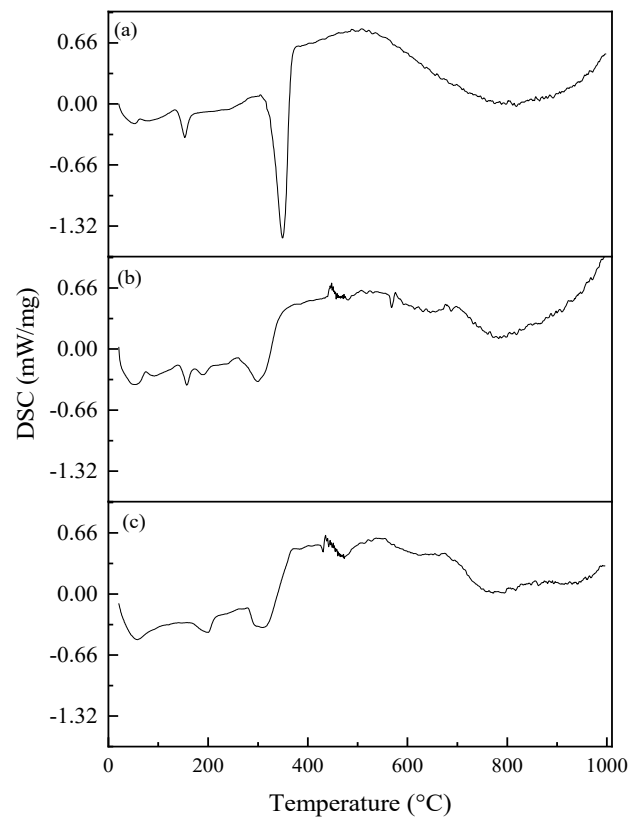


Figure 7. DSC curves of electrospun membranes: (a) PLA; (b) PVA-BIO-HA; (c) PLA/PVA-BIO-HA.

Table 1. Elemental composition of the composite membrane analyzed by EDS.

Element	wt%
C	58.79
O	41.01
P	0.07
Ca	0.14

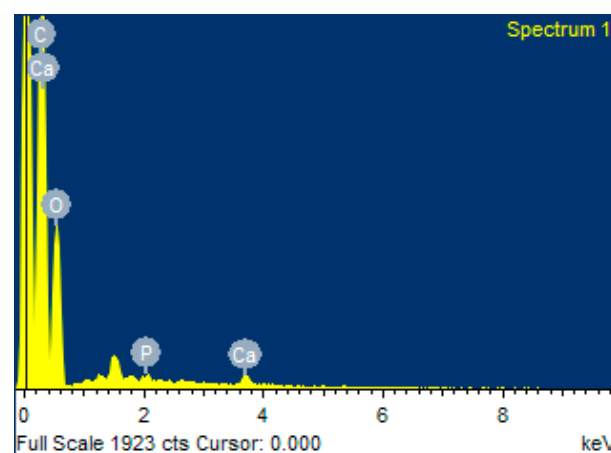


Figure 8. EDS spectrum of the composite membrane.

3.3. Characterization Proliferation, Cytotoxicity

Figure 9 shows the obtained results of the cellular proliferation behavior of PLA/PVA-BIO-HA membranes compared to the proliferation observed in the control group. Significant differences in statistical analyses ($p < 0.05$) are observed between the membrane group

and the control group at 6, 24, and 72 h. These differences can be attributed to enhanced cellular interaction and improved physical support provided by the polymeric membrane acting as a scaffold and the hydroxyapatite particles [25]. It is worth mentioning that after 12 h and 48 h, no significant changes were recorded compared to the control group, and the growth rate was like that of the control group. This can be attributed to the time it takes for cells to properly adhere to and initiate the proliferative process.

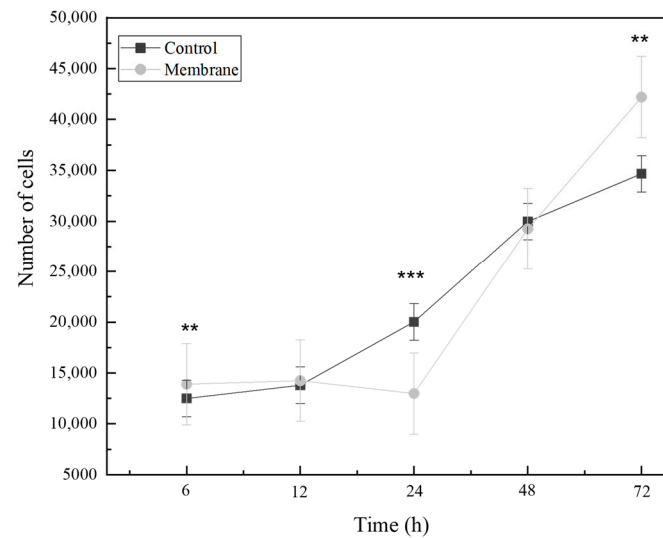


Figure 9. Effect of the composite membrane on the proliferation rate of mesenchymal cells. Time points represent the mean of triplicates (** = $p < 0.01$, *** = $p < 0.001$).

The fluorescence test reveals that human fluorescence-green mesenchymal cells adhere to the polymeric membrane fibers immersed in the cell culture medium over a period of 6, 12, 24, and 48 h. These results demonstrate that the membrane does not induce toxicity in cell culture and supports cell proliferation as a scaffold (Figure 10).

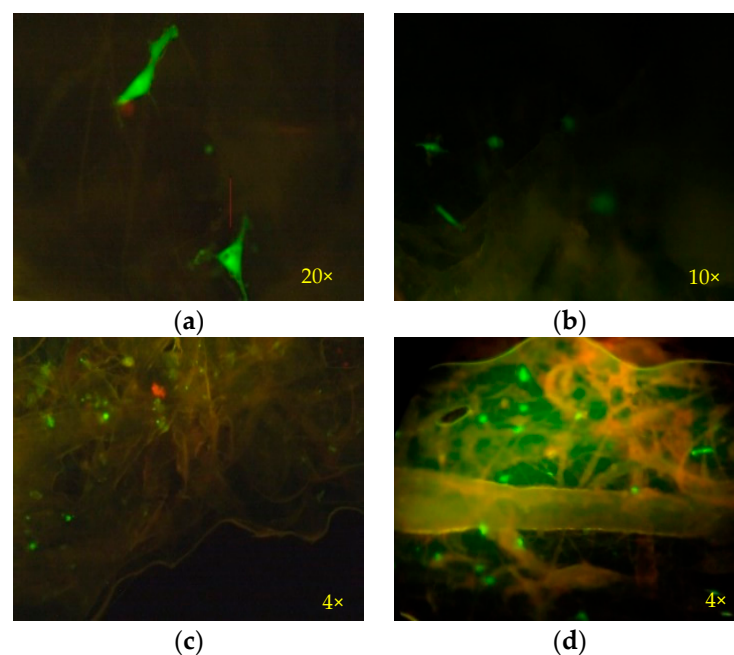


Figure 10. Fluorescence microscopy images obtained from the mesenchymal cell culture medium in contact with polymeric membranes of PLA-PVA-HA: (a) 6 h; (b) 12 h; (c) 24 h; (d) 48 h. Live and attached cells are represented in green on the membrane. The hydroxyapatite agglomerations fluoresce red. The membrane fibers are shown in combination of both green and red colors.

4. Conclusions

In this work, a membrane composed of PLA, PVA, and BIO-HA was fabricated using the coaxial electrospinning technique with a rotating drum. The fabrication was carried out by mixing PLA with TCM, a second solution of PVA with IPA, and BIO-HA. The BIO-HA particles were obtained through the calcination of bovine bone, a process that included cleaning, drying, thermal treatment, and grinding.

FTIR spectroscopy studies confirmed the presence of functional group characteristics in BIO-HA and the polymeric components of PLA and PVA, showing a mixture of whole components in the composite membrane. Also, morphological analyses presented a membrane with randomly arranged fibrous structures exhibiting irregular diameters and spacings of different sizes between fibers; these spaces facilitate nutrient diffusion, cell migration, and adhesion cells.

The PLA-PVA polymer blend showed an improvement in the mechanical properties of the membrane. Additionally, by adding BIO-HA, it was observed that the composite membrane showed greater thermal stability compared to the PLA membrane.

According to the cell proliferation assay, the results showed that the polymeric membrane enhances cellular communication by increasing the number of cells at 6, 24, and 72 h upon contact with the membrane. Additionally, studies on the cytotoxicity assay of the PLA/PVA-BIO-HA membrane resulted in non-toxic outcomes, supporting the morphology and cellular adhesion of mesenchymal cells. Therefore, the results obtained in this study suggest that this composite membrane can be utilized for the regeneration of bone and joint tissue due to the favorable impact of both the BIO-HA and the PLA on cell proliferation.

Author Contributions: Conceptualization, M.A.M.-S.; methodology, B.L.A.-R.; validation, M.A.M.-S.; formal analysis, C.L.G.-M. and P.Z.-M.; investigation, B.L.A.-R.; resources, F.G.-R. and M.A.M.-S.; validation, M.A.M.-S.; writing—review and editing, C.L.G.-M., B.L.A.-R. and P.Z.-M.; supervision, F.G.-R. and M.A.M.-S. All authors have read and agreed to the published version of the manuscript.

Funding: This research received no external funding.

Data Availability Statement: Data are contained within the article.

Acknowledgments: The authors thanks to VIEP-BUAP.

Conflicts of Interest: The authors declare no conflicts of interest.

References

1. Kargozar, S.; Singh, R.K.; Kim, H.-W.; Baino, F. “Hard” ceramics for “Soft” tissue engineering: Paradox or opportunity? *Acta Biomater.* **2020**, *115*, 1–28. [[CrossRef](#)] [[PubMed](#)]
2. Cao, S.; Zhao, Y.; Hu, Y.; Zou, L.; Chen, J. New perspectives: In-situ tissue engineering for bone repair scaffold. *Compos. Part B Eng.* **2020**, *202*, 108445. [[CrossRef](#)]
3. Manzini, B.M.; Machado, L.M.R.; Noritomi, P.Y.; da Silva, J.V.L. Advances in Bone tissue engineering: A fundamental review. *J. Biosci.* **2021**, *46*, 17. [[CrossRef](#)]
4. Biswal, T. Biopolymers for tissue engineering applications: A review. *Mater. Today Proc.* **2021**, *41*, 397–402. [[CrossRef](#)]
5. Mazzoni, E.; Iaquina, M.R.; Lanzillotti, C.; Mazziotta, C.; Maritati, M.; Montesi, M.; Sprio, S.; Tampieri, A.; Tognon, M.; Martini, F. Bioactive materials for soft tissue repair. *Front. Bioeng. Biotechnol.* **2021**, *9*, 613787. [[CrossRef](#)] [[PubMed](#)]
6. Senra, M.R.; Marques, M.d.F.V. Synthetic polymeric materials for bone replacement. *J. Compos. Sci.* **2020**, *4*, 191. [[CrossRef](#)]
7. Kashirina, A.; Yao, Y.; Liu, Y.; Leng, J. Biopolymers as bone substitutes: A review. *Biomater. Sci.* **2019**, *7*, 3961–3983. [[CrossRef](#)] [[PubMed](#)]
8. Guo, L.; Liang, Z.; Yang, L.; Du, W.; Yu, T.; Tang, H.; Li, C.; Qiu, H. The role of natural polymers in bone tissue engineering. *J. Control. Release* **2021**, *338*, 571–582. [[CrossRef](#)]
9. Lett, J.A.; Sagadevan, S.; Fatimah, I.; Hoque, M.E.; Lokanathan, Y.; Léonard, E.; Alshahateet, S.F.; Schirhagl, R.; Oh, W.C. Recent advances in natural polymer-based hydroxyapatite scaffolds: Properties and applications. *Eur. Polym. J.* **2021**, *148*, 110360. [[CrossRef](#)]
10. Sharma, B.; Sharma, S.; Jain, P. Leveraging advances in chemistry to design biodegradable polymeric implants using chitosan and other biomaterials. *Int. J. Biol. Macromol.* **2021**, *169*, 414–427. [[CrossRef](#)]
11. Prasad, A. State of art review on bioabsorbable polymeric scaffolds for bone tissue engineering. *Mater. Today Proc.* **2021**, *44*, 1391–1400. [[CrossRef](#)]

12. Chahal, S.; Kumar, A.; Hussian, F.S.J. Development of biomimetic electrospun polymeric biomaterials for bone tissue engineering. A review. *J. Biomater. Sci. Polym. Ed.* **2019**, *30*, 1308–1355. [[CrossRef](#)]
13. Ferreira, F.V.; Otoni, C.G.; Lopes, J.H.; de Souza, L.P.; Mei, L.H.I.; Lona, L.M.F.; Lozano, K.; Lobo, A.O.; Mattoso, L.H.C. Ultrathin polymer fibers hybridized with bioactive ceramics: A review on fundamental pathways of electrospinning towards bone regeneration. *Mater. Sci. Eng. C* **2021**, *123*, 111853. [[CrossRef](#)] [[PubMed](#)]
14. Wang, Z.; Wang, H.; Xiong, J.; Li, J.; Miao, X.; Lan, X.; Liu, X.; Wang, W.; Cai, N.; Tang, Y. Fabrication and in vitro evaluation of PCL/gelatin hierarchical scaffolds based on melt electrospinning writing and solution electrospinning for bone regeneration. *Mater. Sci. Eng. C* **2021**, *128*, 112287. [[CrossRef](#)] [[PubMed](#)]
15. Tolba, E. Diversity of electrospinning approach for vascular implants: Multilayered tubular scaffolds. *Regen. Eng. Transl. Med.* **2020**, *6*, 383–397. [[CrossRef](#)]
16. Liu, J.; Li, T.; Zhang, H.; Zhao, W.; Qu, L.; Chen, S.; Wu, S. Electrospun strong, bioactive, and bioabsorbable silk fibroin/poly (L-lactic-acid) nanoyarns for constructing advanced nanotextile tissue scaffolds. *Mater. Today Bio* **2022**, *14*, 100243. [[CrossRef](#)] [[PubMed](#)]
17. Jain, R.; Shetty, S.; Yadav, K.S. Unfolding the electrospinning potential of biopolymers for preparation of nanofibers. *J. Drug Deliv. Sci. Technol.* **2020**, *57*, 101604. [[CrossRef](#)]
18. Stojanov, S.; Berlec, A. Electrospun nanofibers as carriers of microorganisms, stem cells, proteins, and nucleic acids in therapeutic and other applications. *Front. Bioeng. Biotechnol.* **2020**, *8*, 130. [[CrossRef](#)] [[PubMed](#)]
19. Miszuk, J.; Liang, Z.; Hu, J.; Sanyour, H.; Hong, Z.; Fong, H.; Sun, H. Elastic mineralized 3D electrospun PCL nanofibrous scaffold for drug release and bone tissue engineering. *ACS Appl. Bio Mater.* **2021**, *4*, 3639–3648. [[CrossRef](#)]
20. Cojocar, E.; Ghitman, J.; Stan, R. Electrospun-Fibrous-Architecture-Mediated Non-Viral Gene Therapy Drug Delivery in Regenerative Medicine. *Polymers* **2022**, *14*, 2647. [[CrossRef](#)]
21. Akhmetova, A.; Heinz, A. Electrospinning proteins for wound healing purposes: Opportunities and challenges. *Pharmaceutics* **2020**, *13*, 4. [[CrossRef](#)] [[PubMed](#)]
22. Rafiei, M.; Jooybar, E.; Abdekhodaie, M.J.; Alvi, M. Construction of 3D fibrous PCL scaffolds by coaxial electrospinning for protein delivery. *Mater. Sci. Eng. C* **2020**, *113*, 110913. [[CrossRef](#)] [[PubMed](#)]
23. Kundu, D.; Banerjee, T. Development of microcrystalline cellulose based hydrogels for the in vitro delivery of Cephalexin. *Heliyon* **2020**, *6*, e03027. [[CrossRef](#)] [[PubMed](#)]
24. Teixeira, M.A.; Amorim, M.T.P.; Felgueiras, H.P. Poly(vinyl alcohol)-based nanofibrous electrospun scaffolds for tissue engineering applications. *Polymers* **2019**, *12*, 7. [[CrossRef](#)] [[PubMed](#)]
25. Pelipenko, J.; Kocbek, P.; Kristl, J. Critical attributes of nanofibers: Preparation, drug loading, and tissue regeneration. *Int. J. Pharm.* **2015**, *484*, 57–74. [[CrossRef](#)] [[PubMed](#)]
26. Alharbi, H.F.; Lugman, M.; Khalil, K.A.; Elnakady, Y.A.; Abd-Elkader, O.H.; Rady, A.M.; Alharthi, N.H.; Karim, M.R. Fabrication of core-shell structured nanofibers of poly(lactic acid) and poly(vinyl alcohol) by coaxial electrospinning for tissue engineering. *Eur. Polym. J.* **2018**, *98*, 483–491. [[CrossRef](#)]
27. Li, T.-T.; Zhang, Y.; Ling, L.; Lin, M.C.; Wang, Y.; Wu, L.; Lin, J.H. Manufacture and characteristics of HA-Electrodeposited polylactic acid/polyvinyl alcohol biodegradable braided scaffolds. *J. Mech. Behav. Biomed. Mater.* **2020**, *103*, 103555. [[CrossRef](#)] [[PubMed](#)]
28. Yudaev, P.; Butorova, I.; Chuev, V.; Posokhova, V.; Klyukin, B.; Chistyakov, E. Wound Gel with Antimicrobial Effects Based on Polyvinyl Alcohol and Functional Aryloxycyclotriphosphazene. *Polym. J.* **2023**, *15*, 2831. [[CrossRef](#)] [[PubMed](#)]
29. Fernández-Cervantes, I.; Morales, M.; Agustín-Serrano, R.; Cardenas-García, M.; Pérez-Luna, P.; Arroyo-Reyes, B.; Maldonado-García, A. Polylactic acid/sodium alginate/hydroxyapatite composite scaffolds with trabecular tissue morphology designed by a bone remodeling model using 3D printing. *J. Mater. Sci.* **2019**, *54*, 9478–9496. [[CrossRef](#)]
30. Arbós, A.; Nicolau, F.; Quetgla, M.; Ramis, J.M.; Monjo, M.; Muncunill, J.; Clavo, J.; Gaya, A. Obtención de células madre mesenquimales a partir de cordones umbilicales procedentes de un programa altruista de donación de sangre de cordón. *Inmunología* **2013**, *32*, 3–11. [[CrossRef](#)]
31. Kesmez, Ö. Preparation of anti-bacterial biocomposite nanofibers fabricated by electrospinning method. *J. Turk. Chem. Soc. Sect. A Chem.* **2020**, *7*, 125–142. [[CrossRef](#)]
32. Abifarin, J.; Obada, D.; Dauda, E.; Dodoo-Arhin, D. Experimental data on the characterization of hydroxyapatite synthesized from biowastes. *Data Brief* **2019**, *26*, 104485. [[CrossRef](#)] [[PubMed](#)]
33. Subrahmanya, T.; Arshad, A.B.; Lin, P.T.; Widakdo, J.; Makari, H.; Austria, H.F.M.; Hu, C.-C.; Lai, J.-Y.; Hung, W.-S. A review of recent progress in polymeric electrospun nanofiber membranes in addressing safe water global issues. *RSC Adv.* **2021**, *11*, 9638–9663. [[CrossRef](#)]
34. Fatahian, R.; Mirjalili, M.; Khajavi, R.; Rahimi, M.K.; Nasirizadeh, N. Effect of electrospinning parameters on production of polyvinyl alcohol/polylactic acid nanofiber using a mutual solvent. *Polym. Polym. Compos.* **2021**, *29*, S844–S856. [[CrossRef](#)]
35. Correia, G.; Falcão, J.; Neto, A.C.; Silva, Y.; Mendonça, L.; Barros, A.; Santos-Oliveira, R.; de Azevedo, W.; Junior, S.A.; Santos, B. In situ preparation of nanohydroxyapatite/alginate composites as additives to PVA electrospun fibers as new bone graft materials. *Mater. Chem. Phys.* **2022**, *282*, 125879. [[CrossRef](#)]
36. Lenhert, S.; Meier, M.-B.; Meyer, U.; Chi, L.; Wiesmann, H.P. Osteoblast alignment, elongation and migration on grooved polystyrene surfaces patterned by Langmuir–Blodgett lithography. *Biomaterials* **2005**, *26*, 563–570. [[CrossRef](#)]

37. Shi, R.; Xue, J.; He, M.; Chen, D.; Zhang, L.; Tian, W. Structure, physical properties, biocompatibility and in vitro/vivo degradation behavior of anti-infective polycaprolactone-based electrospun membranes for guided tissue/bone regeneration. *Polym. Degrad. Stab.* **2014**, *109*, 293–306. [[CrossRef](#)]
38. Cheng, F.-Y.; Wang, S.P.-H.; Su, C.-H.; Tsai, T.-L.; Wu, P.-C.; Shieh, D.-B.; Chen, J.-H.; Hsieh, P.C.-H.; Yeh, C.-S. Stabilizer-free poly(lactide-co-glycolide) nanoparticles for multimodal biomedical probes. *Biomaterials* **2008**, *29*, 2104–2112. [[CrossRef](#)]
39. Murugan, R.; Ramakrishna, S. Aqueous mediated synthesis of bioresorbable nanocrystalline hydroxyapatite. *J. Cryst. Growth* **2005**, *274*, 209–213. [[CrossRef](#)]
40. Rabelo, L.H.; Munhoz, R.A.; Marini, J.; Maestrelli, S.C. Development and characterization of PLA composites with high contents of a Brazilian refractory clay and improved fire performance. *Mater. Res.* **2021**, *25*, e20210444. [[CrossRef](#)]
41. Goma, M.M.; Hugenschmidt, C.; Dickmann, M.; Abdel-Hady, E.E.; Mohamed, H.F.M.; Abdel-Hamed, M. Crosslinked PVA/SSA proton exchange membranes: Correlation between physiochemical properties and free volume determined by positron annihilation spectroscopy. *Phys. Chem. Chem. Phys.* **2018**, *20*, 28287–28299. [[CrossRef](#)] [[PubMed](#)]
42. Hu, Y.; Wang, Q.; Tang, M. Preparation and properties of Starch-g-PLA/poly (vinyl alcohol) composite film. *Carbohydr. Polym.* **2013**, *96*, 384–388. [[CrossRef](#)] [[PubMed](#)]
43. Cestari, F.; Petretta, M.; Yang, Y.; Motta, A.; Grigolo, B.; Sglavo, V.M. 3D printing of PCL/nano-hydroxyapatite scaffolds derived from biogenic sources for bone tissue engineering. *Sustain. Mater. Technol.* **2021**, *29*, e00318. [[CrossRef](#)]

Disclaimer/Publisher's Note: The statements, opinions and data contained in all publications are solely those of the individual author(s) and contributor(s) and not of MDPI and/or the editor(s). MDPI and/or the editor(s) disclaim responsibility for any injury to people or property resulting from any ideas, methods, instructions or products referred to in the content.